



Region-specific deterministic and probabilistic seismic hazard analysis of Kanpur city

ANBAZHAGAN P^{1,2,*}, KETAN BAJAJ¹, NAIRWITA DUTTA¹,
SAYED S R MOUSTAFA^{2,3} and NASSIR S N AL-ARIFI³

¹Department of Civil Engineering, Indian Institute of Science, Bengaluru 560 012, India.

²King Saud University, Riyadh, Saudi Arabia.

³National Research Institute of Astronomy and Geophysics (NRIAG), Cairo 11421, Egypt.

*Corresponding author. e-mail: anbazhagan@civil.iisc.ernet.in

A seismic hazard map of Kanpur city has been developed considering the region-specific seismotectonic parameters within a 500-km radius by deterministic and probabilistic approaches. The maximum probable earthquake magnitude (M_{\max}) for each seismic source has been estimated by considering the regional rupture characteristics method and has been compared with the maximum magnitude observed (M_{\max}^{obs}), $M_{\max}^{\text{obs}} + 0.5$ and Kijko method. The best suitable ground motion prediction equations (GMPE) were selected from 27 applicable GMPEs based on the ‘efficacy test’. Furthermore, different weight factors were assigned to different M_{\max} values and the selected GMPE to calculate the final hazard value. Peak ground acceleration and spectral acceleration at 0.2 and 1 s were estimated and mapped for worst-case scenario and 2 and 10% probability of exceedance for 50 years. Peak ground acceleration (PGA) showed a variation from 0.04 to 0.36 g for DSHA, from 0.02 to 0.32 g and 0.092 to 0.1525 g for 2 and 10% probability in 50 years, respectively. A normalised site-specific design spectrum has been developed considering three vulnerable sources based on deaggregation at the city center and the results are compared with the recent 2011 Sikkim and 2015 Nepal earthquakes, and the Indian seismic code IS 1893.

1. Introduction

Earthquakes are one of the most destructive of natural hazards, having caused huge loss to life and property, from time immemorial. Destruction is not only caused by the collapse of buildings, but also by the compounded influence of landslides, flood, tsunamis and fire that arise due to earthquakes. The Indian subcontinent has also proven to be the origin of many devastating earthquakes such as the 1905 Kangra earthquake ($M_w = 7.8$), the 1950 Assam earthquake ($M_w = 8.5$),

the 2001 Bhuj earthquake ($M_w = 7.7$), the 2005 Kashmir earthquake ($M_w = 7.6$), the 2011 Sikkim earthquake ($M_w = 6.7$) and the 2015 Nepal earthquake ($M_w = 7.8$). The subcontinent may be subjected to more severe earthquakes in the future, due to high seismic strain gaps in the Himalaya region (Kumar *et al.* 2013). The Himalayan subduction zone is considered as a prominent seismic gap and is highlighted as one of the two most seismically active regions in the world, the other being the San Andreas Fault. The highly fertile Indo-Gangetic Plain, bound on its north side by the Himalayas,

Keywords. DSHA; PSHA; maximum magnitude; rupture characteristics; GMPE; SA; PGA.

is supposed to be one of the most populous areas with numerous cities, large and small, lying on it. Rapid development and population growth, along with increasing seismicity, demands seismic microzonation of cities near the Himalayan belt and the Indo-Gangetic Basin (IGB). Therefore, determination of peak ground acceleration (PGA) and response spectra are important for designing buildings, infrastructure projects as well as disaster planning and management.

Seismic hazard estimation is a prime step in seismic microzonation, where micro-level variations of seismic hazard and its effects are quantified and mapped at bedrock level. Kanpur is one of the largest cities lying on the Indo-Gangetic plain, and due to its proximity to the Himalayan Belt is under high seismic risk. Therefore, in this study, an attempt has been made to develop the worst-case deterministic and classical probabilistic seismic hazard map of Kanpur city for 2 and 10% probability of exceedance for 50 years. All the seismic events and sources lying within a 500-km radius of the Kanpur city center were considered based on the past damage distribution of seismic study area (SSA). The maximum magnitude (M_{\max}) from each of the seismic source was estimated using regional rupture characteristics (Anbazhagan *et al.* 2015a) by dividing the whole SSA into two segments based on the seismicity and seismotectonics of SSA. These M_{\max} values were compared with the M_{\max} estimated by maximum magnitude observed (M_{\max}^{obs}), increment of 0.5 to M_{\max}^{obs} and Kijko method. Furthermore, the best suitable ground motion prediction equation (GMPE) for Kanpur SSA has been selected from 27 applicable GMPEs. Segmented GMPEs ranking has been done to select the best suitable GMPE for the present SSA by carrying out ‘efficacy test’ which makes use of Log Likelihood (LLH) given by Scherbaum *et al.* (2009) and Delevalud *et al.* (2009). The deterministic and probabilistic hazard maps were developed for the Kanpur SSA considering the above mentioned regional specific seismotectonic parameters. Probabilistic seismic hazard analysis (PSHA) values were mapped at bedrock level for 2 and 10% probability of exceedance for 50 years. These hazard values are also computed in terms of spectral acceleration at 0.2 and 1 s. Further, deaggregation plot from venerable sources were developed to figure out the hazard percentage from different combinations of magnitude and hypocentral distance. Moreover, a site-specific normalised design spectrum has been developed by both deterministic and probabilistic hazard values (DSHA and PSHA) from the three vulnerable sources at the city center and compared with the 2011 Sikkim earthquake and the Indian standard code (IS 1893 2002).

2. Study area and seismicity

The Indo-Gangetic Basin (IGB) that runs parallel to the seismically active Himalayan Belt is under high risk of seismic hazard. Apart from the seismicity of the Himalayan Belt, the floor of the Gangetic trough is corrugated by inequalities and buried ridges. In addition, the IGB possesses a thick alluvial cover because of which the distant earthquakes have been felt strongly (ASC 2010). Tremors from recent 2016 India–Myanmar border (7.2 M_w) were also felt in Kanpur city center. Some of the active tectonic features lying underneath the Indo-Gangetic Plain are the Delhi–Haridwar Ridge (DHR), the Delhi–Muzaffarnagar Ridge and the Faizabad Ridge (FR). FR runs in a curved manner, first from east to west from Allahabad to Kanpur and then starts to bend towards the north-east towards Lucknow (ASC 2010). Major earthquakes have occurred in the Himalayan region since historic times, some of them being the 1833 Bihar earthquake, 1905 Kangra earthquake, 1934 Bihar–Nepal and the 2011 Sikkim earthquakes; these earthquakes had affected the cities in the IGB. As per Bilham (2015), the Nepal 2015 earthquake has failed to fully rupture the main fault beneath the Himalayan region, hence, a large earthquake is inevitable in the near future.

The study area of Kanpur lies in the central part of the IGB and is surrounded by two main rivers of India, viz., the Ganges in the north-east and Yamuna in the south. Kanpur is the second most populous city of Uttar Pradesh with an approximate population of 2.5 million inhabitants. The city of Kanpur is famous as one of the major industrial belts of India and is popularly known by the nicknames ‘Leather City’ and ‘Manchester of the East’. Kanpur city covers an area of over 605 km² with its central point having latitude 26.46°N and longitude 80.33°E. The study area of Kanpur lies in the Seismic Zone III, as per the current seismic zonation map of India (IS 1893 2002) and has a zone factor of 0.16 for design basis earthquake. As per USGS, weak shaking (macroseismic intensity less than IV) is observed in Kanpur and surrounding areas because of the recent 2015 Nepal earthquake.

Kanpur city being situated in the IGB is surrounded by many inhomogeneities in the form of faults and ridges, like DHR, FR and the Lucknow Fault. Kanpur lies merely 100 km away from Lucknow city, which is located along the Lucknow–Faizabad fault (LFF) and the fault has a seismic gap of 350 years and is capable of a disastrous earthquake, as it is inactive for last 350 years (Nadesha 2004). Because of its inactivity since many years, researchers have highlighted that this fault has been under heavy stress and hence has

the potential to cause a massive earthquake in the future. With the Himalayan rise due to the subduction of the Indian plate under Eurasian plate, movement of the Indian plate by 5.25 m could cause a large earthquake on the Faizabad fault as per Earthquake Mitigation Department, Government of Uttar Pradesh (Nadesha 2004).

Besides being surrounded by several faults and ridges, Kanpur also lies within a distance of 400 km from the two active thrusts – Main Boundary Thrust (MBT) and the Main Central Thrust (MCT), which are present along the entire Himalayan tectonic belt and have a history of devastating earthquakes. Though there is no history of recorded earthquake data in which Kanpur is found to be the epicentre, many earthquakes have taken place within a 300-km radius of the city center, like the 1925 Sultanpur earthquake ($M_L = 6$), 1961 Kheri earthquake ($M_L = 6$) and the 1965 Gorakhpur earthquake ($M_L = 5.7$) (ASC 2010). Past historical evidences show that the 1803 Nepal earthquake caused an intensity of VI (MSK scale) and the 1833 Nepal earthquake caused an intensity of V–VI (Rossi Forel scale), both having epicentres within a 600-km distance of Kanpur city center (Kayal 2008). By taking into consideration the above seismic sources and the events that took place in and around Kanpur city, it can be concluded that this urban city is under a high risk of seismic hazard due to future earthquakes. Therefore, an attempt has been made in this study to estimate the worst-case seismic hazard parameters at the bedrock level for Kanpur city due to surrounding seismic features.

3. Seismotectonic map

In order to quantify the seismic hazard of an area, information about the active seismic features such as faults, lineaments and shear zones and all the earthquake events need to be compiled in the form of a map, which is known as a seismotectonic map. For generating a seismotectonic map of the SSA, researchers have considered various radial distances from the urban city center and validated the same by accounting many factors. By studying the seismicity of the Kanpur region and the past damage distribution map of 1803 Nepal earthquake (Ambraseys and Douglas 2004), a radial extent of 500 km is taken from the Kanpur city center.

In the present study, for the preparation of seismotectonic map, linear sources were taken from the Seismotectonic Atlas of India produced by the Geological Survey of India (GSI 2000). These maps were scanned using a high-resolution scanner, digitised for identification of the linear sources, considering a 500-km radius from Kanpur city center and

was verified with the seismotectonic map prepared by Kolathayar *et al.* (2012) for the whole India and Kumar *et al.* (2013) for Lucknow region. No aerial source has been considered in this study since, as good distributions of linear sources were available for the study area.

Data of all the past earthquake events around a 500-km radial distance of Kanpur city center were collected from different sources such as the National Earthquake Information Centre, International Seismological Centre, Indian Meteorological Department, United State Geological Survey, Northern California Earthquake Data Centre, and the Geological Survey of India. A total of 3140 events were collected, providing details of the events like epicentre coordinates, year, month, date, focal depth and magnitudes in different magnitude scales. Since the magnitudes of the events collected were in different magnitude scales, like body wave magnitude, Richter or local magnitude, surface wave magnitude and moment magnitude (M_w), they were all converted into M_w for consistency and homogeneity. A series of empirical relationships have been developed between these magnitudes by various researchers, but for this study, the relationship developed by Scordilis (2006), which included the worldwide data, was used.

Declustering is considered necessary for seismic hazard assessment and other applications in seismology, such as the development of earthquake prediction models for achieving the best result of hazard analysis (Wiemer and Wyss 1994, 1997) and for seismicity rate change estimation (Frankel 1995). For the present study, the declustering algorithm developed by Gardner and Knopoff (1974) and modified by Uhrhammer (1986) was used. This algorithm assumes that the time and spatial distribution of the foreshocks and aftershocks depend on the magnitude of the main event. As per the study by Stiphout *et al.* (2010), seismicity background derived by the method of Gardner and Knopoff (1974) follows a Poisson distribution, whereas the static window method (Reasenber 1985) does not. Out of 3140 events, around 50% were found to be dependent events; 1576 events were acknowledged as the main shock. These events along with linear seismic sources were compiled for the preparation of the seismotectonic map. The complete catalogue contains 918 events with $M_w < 4$; details of events with $M_w > 4$ are summarised in table 1. In order to develop the seismotectonic map, declustered earthquake events were superimposed with the source map, as shown in figure 1. It is seen from figure 1 that events are more densely located near MBT and MCT as compared to the other areas. Therefore, the whole seismotectonic map was divided into two regions using a trapezoid – Region I (which covers the events lying inside the trapezoid

Table 1. Summary of events having M_w greater than or equal to 4.

Sl. no.	Earthquake magnitude (M_w) range	Number of events	
		Region I	Region II
1	$4 \leq M_w < 4.5$	51	34
2	$4.5 \leq M_w < 5$	214	87
3	$5 \leq M_w < 5.5$	120	47
4	$5.5 \leq M_w < 6$	37	17
5	$6 \leq M_w < 6.5$	25	12
6	$6.5 \leq M_w < 7$	5	3
7	$M_w \geq 7$	2	4

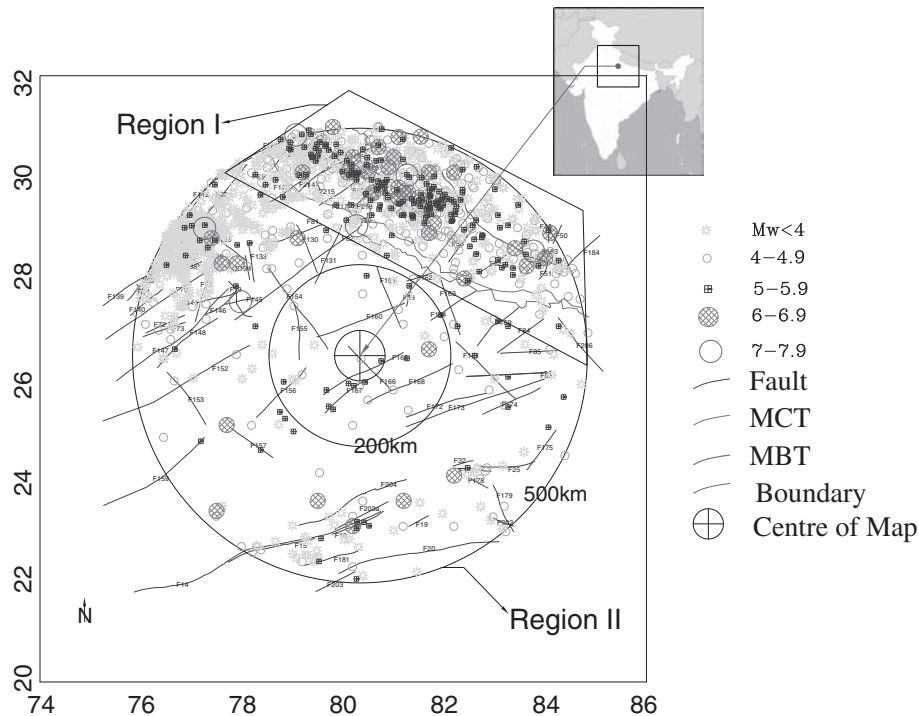


Figure 1. Seismotectonic map of Kanpur.

and envelopes MBT and MCT) and Region II (which covers events outside the trapezoid). Analysis was carried out for both the regions separately.

4. Data completeness and G–R recurrence relationship

Seismic parameters should be evaluated for the determination of the seismic hazard map and estimating the ground motions due to future earthquakes. These parameters include a and b parameters of the Gutenberg–Richter (G–R) recurrence relations (Gutenberg and Richter 1956). A complete earthquake catalogue is needed for presenting the seismicity pattern of a region and this, in turn, is required to be analysed for carrying out the seismic hazard analysis of a region. The seismic parameters around Kanpur site for Regions I and II

can be quantified by the standard Gutenberg–Richter (G–R) recurrence relationship (Gutenberg and Richter 1956). The seismic recurrence rate can be assessed correctly if the collected data of the earthquake events are complete. Therefore, the composed data of Kanpur SSA is scrutinised for its completeness using the graphical method proposed by Stepp (1972). Anbazhagan *et al.* (2009) described the detailed procedure for completeness analysis as per Stepp (1972). Based on the analysis, it can be summarised that the earthquake catalogue for the Region I has been completed for the last 60 years for a magnitude moment <5.0 and for last 80 years for higher magnitudes. For Region II, the earthquake catalogue for magnitude <5.0 is complete for the last 60 years and completed for 80 years for higher magnitudes. The a and b parameters were determined for both the regions for the complete data. Figure 2 shows the G–R recurrence

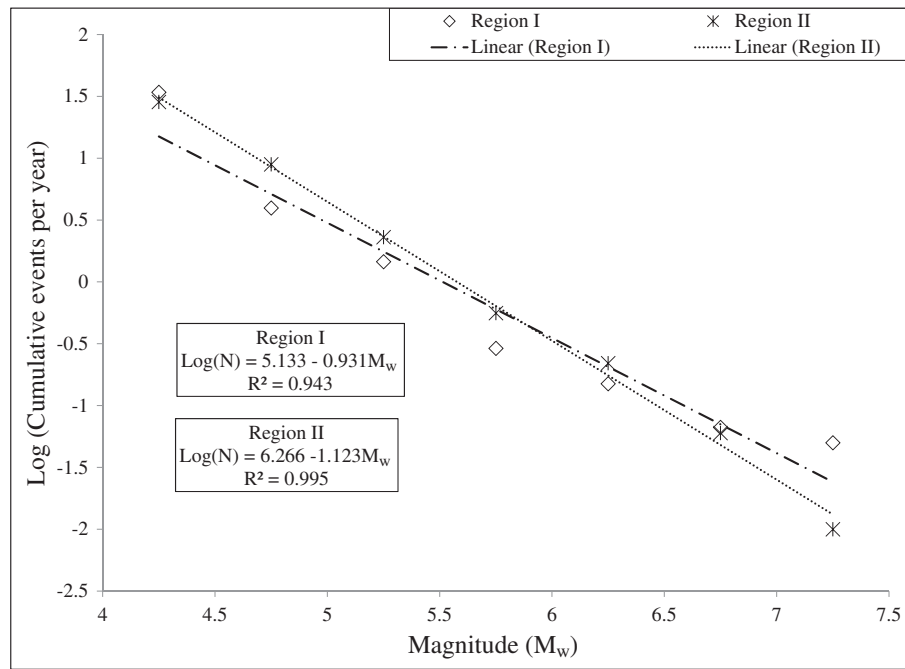


Figure 2. Gutenberg–Richter relation for Regions I and II.

Table 2. Comparison of ‘b’ parameter of the present study with previous data.

Region I	Region II
0.93 (Present work)	1.12 (Present work)
0.91 (Anbazhagan <i>et al.</i> 2015b)	1.01 (Anbazhagan <i>et al.</i> 2015b)
0.86 (Kumar <i>et al.</i> 2013)	0.80 (Kumar <i>et al.</i> 2013)
0.73 (NDMA 2010)	0.81 (NDMA 2010)
1.0 (Sreevalsa <i>et al.</i> 2011)	0.85 (Sreevalsa <i>et al.</i> 2011)
0.80 (Mahajan <i>et al.</i> 2010)	0.92 (Shanker and Sharma 1998)
0.65 (Kumar 2012)	
0.92 (Shanker and Sharma 1998)	
0.96 (Yadav <i>et al.</i> 2011)	

law for Regions I and II, with a correlation coefficient of 0.94 and 0.99, respectively. The *b* value for the Region I is 0.93 and for Region II is 1.12. The values obtained are comparable with the earlier studies performed by other researchers (see table 2). These values were further used for estimating the maximum magnitude and for probabilistic seismic hazard analysis of Kanpur city.

5. Maximum probable earthquake (M_{max}) and focal depth

Since the complete earthquake catalogue of any region represents only a small portion of the total seismic activity, it is difficult to estimate the complete potential of any region or source for future seismicity. It is the upper limit of earthquake magnitude for a given seismogenic zone or the entire region and is synonymous with the magnitude

of the largest possible earthquake in that region (EERI 1984; WGCEP 1995). It assumes a sharp cut-off magnitude at a maximum magnitude, so by definition, no earthquake is to be expected with magnitude exceeding M_{max} (Joshi and Sharma 2008).

In the present study, M_{max} is estimated using regional rupture characteristics by considering the maximum magnitude observed magnitude (M_{max}^{obs}) and possible seismic source. Anbazhagan *et al.* (2015a) found that regional rupture character is unique and does not change with seismic study area. Rupture character of the region was derived by considering earthquake moment magnitude (M_w) of 4.8 and above and the associated subsurface rupture length (RLD). RLD of each seismic source has been estimated by using the well accepted correlation between RLD and M_w by Wells and Coppersmith (1994) for the determination of maximum observed magnitude of each source. The

correlation given by Wells and Coppersmith (1994) between RLD and M_w is valid for moment magnitude from 4.8 to 8.1. Percentage fault rupture (PFR) is the ratio of RLD to total fault length (TFL) and is expressed in percentage. As the present study area is lying at a distance of 400 km from MBT and MCT and hazard characteristics are affected mainly by seismicity within 200 km of any SSA, so an advanced procedure for the determination of M_{max} using regional rupture characteristics for seismically active zone is presented in the present study. The M_{max} calculated is compared with M_{max}^{obs} , increment of 0.5 to M_{max}^{obs} and Kijko method.

The Kanpur SSA has been divided into two radii of consideration, viz., 0–200 km and further 200–500 km based on seismicity and seimotectonics (see figure 1). As per figure 3, the plotting of PFR against TFL showed that PFR follows a unique trend for the interplate region. It can be observed from figure 3 that the percentage of the total fault ruptured for shorter faults is more when compared to that of the longer faults, showing a decreasing

trend with an increase in the fault length. This indicates that most of the damaging earthquakes in the region follow the same trend. The PFR of the worst possible scenario was established by considering minimum, maximum and average PFR in four length bins as shown in table 3 for both the segments. PFR for the worst-case scenario (table 3) was taken as the regional rupture character of the SSA. The RLD was calculated based on the TFL for each source, which was further used to estimate the respective M_{max} using a well-established Wells and Coppersmith (1994) relationship. The absolute M_{max} for each source was calculated using the above-mentioned approaches. The range of the M_{max} estimated from the regional rupture characteristic of Kanpur SSA, considering two different radii, is 5.5–6.2 M_w upto 200 km and 5.7–7.3 M_w for 200–500 km, respectively. M_{max} estimated from the above method is compared with M_{max}^{obs} , increment of 0.5 to M_{max}^{obs} and Kijko method. M_{max}^{obs} for 200- and 500-km radii is 6.2 and 7.1 M_w , so $M_{max} = M_{max}^{obs}$. M_{max} of 6.7 M_w for 200 km and 7.6 M_w for 200–500 km can be determined as per

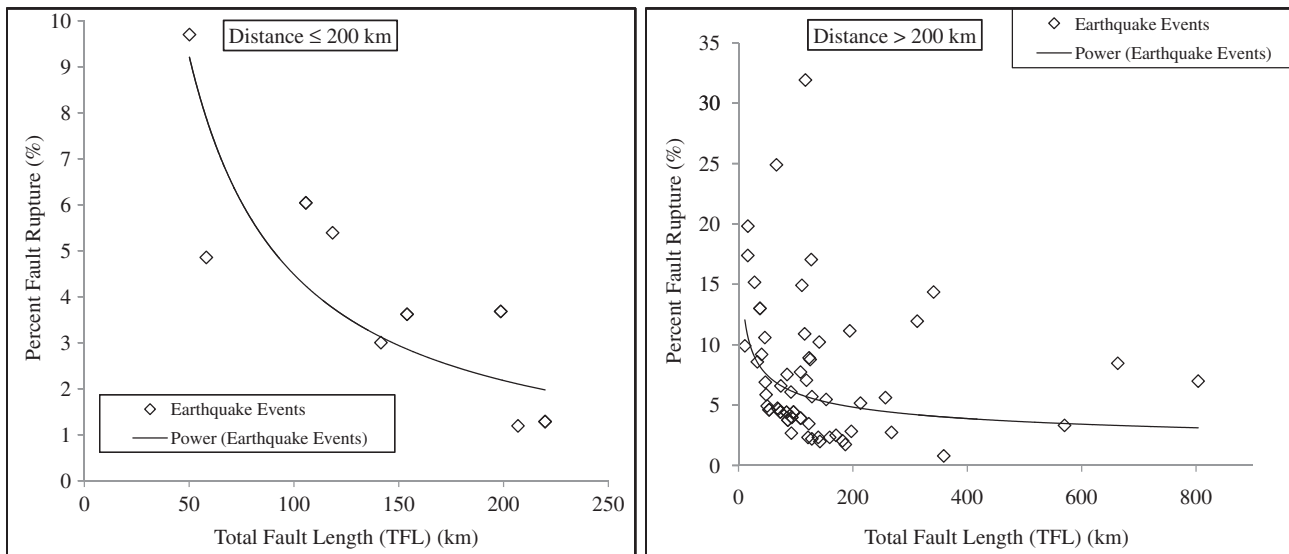


Figure 3. Regional rupture character for subsurface rupture length in terms of percent of total length of fault versus total length of fault for Kanpur for 200 km and 200–500 km.

Table 3. Regional rupture character for various distance bins.

Maximum	PFR (% TFL)		PFR (% TFL) for worst scenario (WS)	Ratio of PFR for WS to maximum PFR
	Minimum	Average		
Dist. ≤ 200 km				
9.69	4.11	5.79	12	1.24
3.68	1.97	2.44	5	1.36
Dist. > 200 km				
31.9	1.98	8.58	35	1.10
14.36	1.72	5.65	15	1.04
8.46	0.78	4.88	10	1.18

$M_{\max} = M_{\max}^{\text{obs}} + 0.5$, which is generally used by various researchers in India. Furthermore, M_{\max} is also estimated using Kijko and Sellevoll (1989), which considers the doubly truncated Gutenberg-Richter relationship. The range of the M_{\max} estimated from Kijko and Sellevoll (1989) for Kanpur site for two different radii of consideration are 5.0–6.5 M_w for 200 km and 4.1–7.1 M_w for 200–500 km, respectively. Table 4 gives the M_{\max} value from the seismic source having an estimated maximum observed moment magnitude greater than 7.0. The maximum magnitude is over-estimated for some of the seismic sources, as calculated from $M_{\max} = M_{\max}^{\text{obs}} + 0.5$. Furthermore, in some of the seismic sources, maximum magnitude was found to be the maximum observed magnitude when calculated using the method of Kijko and Sellevoll (1989). By analysing the error and uncertainty in all the methods, different weight factors, i.e., 0.4, 0.2, 0.2 and 0.2 were assigned to maximum magnitude calculated from regional rupture characteristics, $M_{\max} = M_{\max}^{\text{obs}}$, $M_{\max} = M_{\max}^{\text{obs}} + 0.5$ and Kijko and Sellevoll (1989) method, respectively. The weighting factors in all the methods are explained in Anbazhagan *et al.* (2015a). Therefore, in the present study, PGA values for Kanpur SSA were calculated by assigning different weight factor to M_{\max} estimate from each of the above-mentioned methods.

Based on the present methods, it can be seen that the calculated M_{\max} for MCT and MBT is 7.2 and 7.3, respectively, as the segment of MCT and MBT considered in the SSA has M_{\max}^{obs} 7.1. However, most of the seismologists believe that a central seismic gap exists between the 1905 Kangra earthquake and 1935 Bihar Nepal earthquake, which has the potential of experiencing a great earthquake

($M_w > 8$) in near future. Hence, in the present study, a maximum magnitude of 8.3 M_w was considered for determining the hazard values in the Kanpur city, since M_{\max}^{obs} in the entire length of MBT is 8.1 M_w (1934 Bihar Nepal Earthquake). A recent study carried out by Yadav *et al.* (2011) on the assessment of earthquake hazard parameters in the north-west Himalaya, also calculated the M_{\max} for the same region as 8.3 M_w . Therefore, the M_{\max} of 8.3 for both MBT and MCT has been considered for further hazard assessment for Kanpur city.

5.1 Focal depth of earthquake

A critical part of seismic hazard analysis is the determination of the focal depth of earthquakes. The depth division of the diffuse seismicity (i.e., derived from the seismology database) should be included in the seismic hazard analysis (IAEA SGS-9 2010). Most of the studies regarding the seismic hazard analysis incorporate the lowest focal depth or depth considering the minor earthquakes (Anbazhagan *et al.* 2013b). In the present study, the whole catalogue has been analysed for determination of the appropriate focal depth of the future earthquake. It was analysed with the magnitude and epicentral distance for the Kanpur SSA. Depth versus epicenter distance of events having a M_w greater than 5 for Kanpur region was studied and analysed statistically and given as figure 4. It was found that for all magnitude values with a moment magnitude >5 , the focal depth varied from 10 to 75 km (see figure 4). So, considering the worst-case scenario, a focal depth of 15 km was adopted for events with $M_w < 5$, 30 km for $5 \leq M_w < 6.5$ and 50 km for $M_w \geq 6.5$, for both deterministic and probabilistic hazard analyses.

Table 4. Estimation of M_{\max} for each seismic source used in the study considering four approaches.

Fault name	Rupture characteristics			$M_{\max} = M_{\max}^{\text{obs}}$	$M_{\max} = M_{\max}^{\text{obs}} + 0.5$	Kijko and Sellevoll (1989)	Final M_{\max}
	TFL (km)	RLD (% TFL)	M_{\max} by rupture				
MBT	803.74	72.34	7.3	7.1	7.6	7.1	8.3*
MCT	663.07	59.68	7.1	7.1	7.6	7.1	8.3*
F82	341.03	51.15	7.0	7.1	7.6	7.0	7.1
F135	116.96	38.60	6.8	7.1	7.6	6.5	7.0
F62	312.49	46.87	7.0	7.1	7.6	6.1	7.0
F125	127.17	41.96	6.9	7.1	7.6	6.4	7.0
F126	194.48	29.17	6.6	7.1	7.6	6.4	6.9
F14	570.05	51.30	7.0	7.1	7.6	6.3	7.0
F136	66.36	21.90	6.4	7.1	7.6	6.3	6.8
F157	110.75	36.55	6.8	7.1	7.6	6.2	6.9
F124	141.12	46.57	7.0	7.1	7.6	6.0	6.9
F204	256.90	38.53	6.8	7.1	7.6	6.0	6.9

*Final M_{\max} calculated is 7.3 and 7.2 for MBT and MCT, however, 8.3 is considered for hazard assessment (explanation is given in the text).

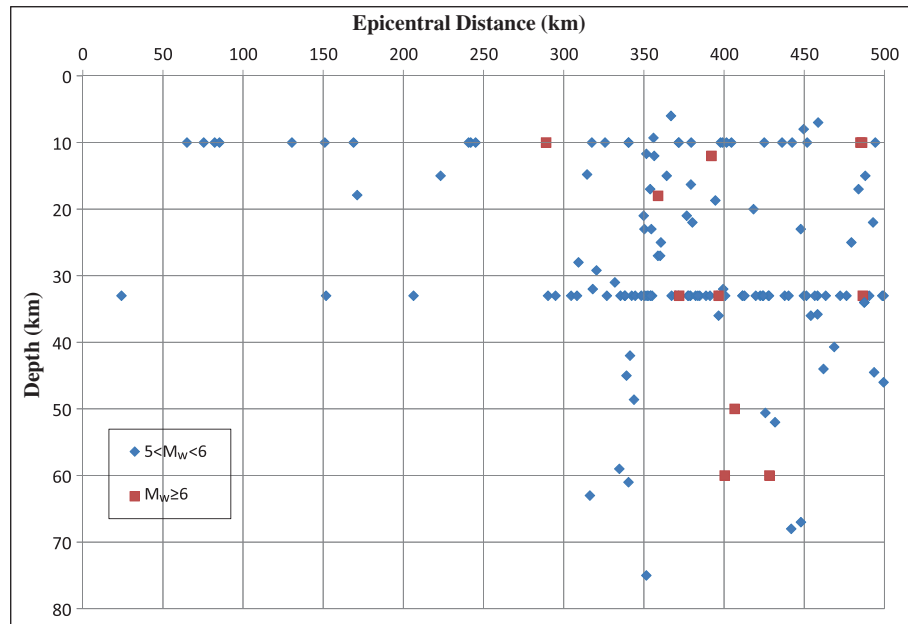


Figure 4. Distribution of focal depth of earthquake with epicentral distance.

6. Ground motion prediction equation (GMPE)

The ground motion prediction equation provides a means of predicting the level of ground shaking and its associated uncertainty at any given site or location, based on the earthquake magnitude, site to source distance, local soil conditions, fault mechanism, etc. Region-specific GMPE is an important component for seismic hazard analysis for both seismic macro- and micro-zonation. Selection of an appropriate GMPE is an indispensable step in determining the ground motion due to an earthquake and for carrying out seismic hazard analysis. However, a limited number of region-specific GMPEs are available for India and other parts of the world, for seismic hazard estimation, both at the bedrock level, as well as at the surface level, which considers the local site effects (Atkinson and Boore 2006; NDMA 2010). At the same time, developed countries are working on Next Generation Attenuation (NGA) for the better estimation of ground motions and prediction of ground shaking for earthquake resistant design of structures (Campbell and Bozorgnia 2006; Kaklamanos and Baise 2011).

Various researchers have analysed the attenuation characteristics of the Himalayan region based on the past available data. Region-specific GMPEs for India were developed by various researchers, based on the recorded as well as simulated earthquake data and are given in table 5 (1–11). In addition to these GMPEs, there are several GMPEs developed for similar tectonic which were found to be applicable to the Himalayan region. The list of

GMPEs applicable for the study region along with abbreviations is given in table 5 (12–27). Details regarding all the GMPEs have been submitted as an electronic material in Anbazhagan *et al.* (2015b). All the GMPEs used in the present study are at bedrock level with shear wave velocity more than 1500 m/s. Many researchers in India generally use two or three GMPEs for predicting the hazard values. However, considering 2–3 GMPEs randomly and comparing with the observed value may give inconsistent results because of the absence of an organised, logical and comprehensive procedure. Hence, for the present study area, the best suitable GMPE was selected for hazard analysis by considering past earthquake data.

The best suitable GMPE was selected considering the criteria proposed by Bommer *et al.* (2010) and by performing the efficacy test recommended by Scherbaum *et al.* (2009) and Delevalud *et al.* (2009). The determination of the order of ranking of GMPEs was based on the observed earthquakes in a particular region. In the present study, the information-theoretic approach recommended by Scherbaum *et al.* (2009) has been used. The efficacy test makes use of average sample log-likelihood (LLH) for the ranking purpose of the available GMPE of a particular SSA. The efficacy test using an average LLH has been performed successfully by Delevalud *et al.* (2009) and further applied to the Indian subcontinent by Nath and Thingbaijam (2011) and Anbazhagan *et al.* (2016). Hence, for the present study, efficacy test has been carried out by considering the Macroseismic Intensity Map of 1803 Nepal earthquake and PGA-European Macroseismic Scale (EMS, Grünthal 1998) relation

Table 5. Available GMPEs with their abbreviations considered for the seismic study area.

Sl. no.	Ground motion prediction equation (GMPE)	Abbreviation of the equations
1	Singh <i>et al.</i> (1996)	SI-96
2	Sharma (1998)	SH-98
3	Nath <i>et al.</i> (2005)	NATH-05
4	Das <i>et al.</i> (2006)	DAS-06
5	Sharma and Bungum (2006)	SHBU-06
6	Baruah <i>et al.</i> (2009)	BA-09
7	Nath <i>et al.</i> (2009)	NATH-09
8	Sharma <i>et al.</i> (2009)	SH-09
9	Gupta (2010)	GT-10
10	National Disaster Management Authority (2010)	NDMA-10
11	Anbazhagan <i>et al.</i> (2013a)	ANBU-13
12	Abrahamson and Litehiser (1989)	ABLI-89
13	Youngs <i>et al.</i> (1997)	YONG-97
14	Campbell (1997)	CAMP-97
15	Spudich <i>et al.</i> (1999)	SPUD-99
16	Atkinson and Boore (2003)	ATKB-03
17	Takahashi <i>et al.</i> (2004)	TAKA-04
18	Ambraseys <i>et al.</i> (2005)	AMB-05
19	Kanno <i>et al.</i> (2006)	KANO-06
20	Zhao <i>et al.</i> (2006)	ZHAO-06
21	Campbell and Bozorgnia (2008)	CABO-08
22	Idriss (2008)	IDRS-08
23	Boore and Atkinson (2008)	BOAT-08
24	Abrahamson and Silva (2007)	ABSI-08
25	Aghabarati and Tehranizadeh (2009)	AGTE-08-09
26	Lin and Lee (2008)	LILE-08
27	Akkar and Bommer (2010)	AKBO-10

proposed by Nath and Thingbaijam (2011) for Indian crustal earthquakes. Based on the validity of particular GMPE, the hypocentral distance was divided into three length bins, viz., 0–100 km, 100–300 km and 300–500 km. For the hazard analysis, the ranking of GMPE has been considered for all the three bins. Some of the GMPEs such as Singh *et al.* (1996), Sharma (1998), Das *et al.* (2006), Baruah *et al.* (2009), Sharma *et al.* (2009) and Gupta (2010) were not used for efficacy test because the isoseismal map used in the present study area has a moment magnitude of 7.7 and these GMPEs are only applicable for moment magnitude < 7.7. The LLH values along with the ranking of GMPEs are given in table 6. The EMS values were used to estimate the LLH values and Data Support Index (DSI), which were further used to rank the GMPEs. Segment-based ranking of GMPEs has been attempted in order to avoid over/underestimation of PGA at shorter and longer distances. In order to select best suitable GMPEs for each region/past earthquake location, DSI criteria are given by Delavaud *et al.* (2012) has been used. For each distance segment, positive DSI values were calculated and ranked based on maximum to

minimum values. The maximum positive DSI value was given the first rank and the minimum was considered as the lowest rank. Segmental analysis of available GMPEs for SSA has been done and the positive DSI values for Kanpur earthquake is marked in bold in table 6. Details regarding LLH, DSI and weight calculation for various GMPEs has been given in Anbazhagan *et al.* (2015b and 2016). From the efficacy test, it has been seen that 6 GMPEs such as ABSI-08, ANBU-13, NDMA-10, KANO-06, NATH-05 and BOAT-08 can be used up to a hypocentral distance of 100 km. For distances of 100–300 km, KANO-06, ANBU-13, NDMA-10 and BOAT-10 can be used, and for a hypocentral distance >300 km, NDMA-10 can be used for the hazard analysis. The plot of GMPE used in this study for varied distance bin is shown in figure 5(a). The selected GMPEs are also compared with the recent Nepal 2015 earthquake records and shown in figure 5(b). The recorded data for Nepal 2015 earthquake is collected from Chadha *et al.* (2016). The main shock was recorded at 18 stations in the distance range of 270–1000 km. Out of 18 recording stations, 14 are at soil site and 4 are at rock site. Chadha *et al.* (2016) classified these sites as site

Table 6. Segmented Ranking of GMPEs for Kanpur Region.

Sl. no.	GMPEs	0-100				100-300				300-500			
		LLH	DSI	R*	W [#]	LLH	DSI	R*	W [#]	LLH	DSI	R*	W [#]
1	ABLI-89_Hort	6.227	-85.641	10	-		NA				NA		
2	ABLI-89_Vert	10.462	-99.237	22	-		NA				NA		
3	YONG-97	7.217	-92.767	15	-	10.462	-87.584	5	-	5.430	-74.697	2	-
4	CAMP-97_Hort	4.321	-46.156	7	-		NA				NA		
5	CAMP-97_Vert	6.276	-86.116	11	-		NA				NA		
6	SPUD-99	10.188	-99.077	21	-		NA				NA		
7	TAKA-04	6.934	-91.198	13	-	12.937	-97.767	7			NA		
8	AMB-05	9.307	-98.301	16	-		NA				NA		
9	NATH-05	2.881	46.068	5	0.08		NA				NA		
10	KANO-06	1.523	274.311	4	0.18	5.441	303.055	1	0.34		NA		
11	ZHAO-06	6.934	-91.198	14	-	12.937	-97.767	8	-		NA		
12	SHBU-06	91.097	-100	23	-	41.615	-100	12	-		NA		
13	IDRS-08	8.155	-96.224	16	-	21.905	-99.995	10	-		NA		
14	BOAT-08	3.027	31.963	6	0.07	5.850	63.240	3	0.19	10.320	-98.310	4	-
15	ABSI-08	1.098	402.715	1	0.23	10.847	-90.493	6	-		NA		
16	CABO-08	6.644	-89.243	12	-	23.934	-99.998	11	-		NA		
17	LILE-08	8.949	-97.823	17	-	14.042	-98.962	9	-	6.505	-87.991	3	-
18	AGTE-08-09_Vert	5.756	-80.087	8	-		NA				NA		
19	AGTE-08-09_Hort	5.071	-68.002	9	-		NA				NA		
20	NATH-09	9.804	-98.796	20	-		NA				NA		
21	AKBO-10	9.356	-98.358	19	-		NA				NA		
22	NDMA-10	1.213	364.069	3	0.21	6.315	119.919	4	0.18	1.608	257.769	1	1
23	ANBU-13	1.108	399.104	2	0.23	5.692	238.692	2	0.29		NA		

R*: ranking of GMPE, W[#]: weight of GMPE having positive DSI.

class B, C, D and E by comparing the recording with GMPE developed by Atkinson and Boore (2003). The same seismic site class has mentioned in figure 5(b) for comparison. It can be seen from figure 5(b) that the selected GMPEs are matching with rock data, i.e., site class A and B. However, site class C and D, PGA values are much above the selected GMPE values due to local site effects. In the present study, DSI were directly calculated using LLH and weight were calculated later from only those GMPE that are having positive DSI (table 6). The weight factor corresponding to particular GMPE for different segments was further used in evaluating the hazard of Kanpur SSA. Seismic hazard values in terms of PGA and SA will be calculated considering these equations for each seismic source.

7. Hazard maps for Kanpur region

To derive the hazard value in terms of PGA and SA for 0.2 and 1 s time period, both, deterministic seismic hazard analysis (DSHA) and probabilistic seismic hazard analysis (PSHA) were used. The detailed procedures for both the methods are explained in Anbazhagan *et al.* (2009) and Kumar

et al. (2013). The calculated PGA values at bedrock level will be useful in site response of ground motion parameters and liquefaction assessment in future for Kanpur SSA. For deriving the hazard map, GMPE has been selected and weights based on the regional data. The weight factors of 0.23, 0.23, 0.21, 0.18, 0.08 and 0.07 for ABSI-08, ANBU-13, NDMA-10, KANO-06, NATH-05 and BOAT-08, respectively, up to 100 km were used. GMPEs of KANO-06, ANBU-13, NDMA-10 and BOAT-10 were assigned factors 0.34, 0.29, 0.19 and 0.18 for a segmented hypocentral distance of 100–300 km and a factor of 1 for NDMA-10 for more than 300 km hypocentral distance were used. For determining the PGA deterministically and probabilistically, by considering magnitude, source-to-site distance and site condition, (shear wave velocity more than 1500 m/s) MATLAB code has been generated. Validation of the code was done with the results of EM-1110 (1999). The whole Kanpur city's SSA was divided into 635 grids of size $0.02^\circ \times 0.02^\circ$ along the longitude and latitude, respectively. The following procedure was used to determine the PGA value for each of the 635 grids. For the development of the seismic hazard map, both deterministically and probabilistically, the Kriging interpolation technique was used for the estimation of intermediate values of PGA.

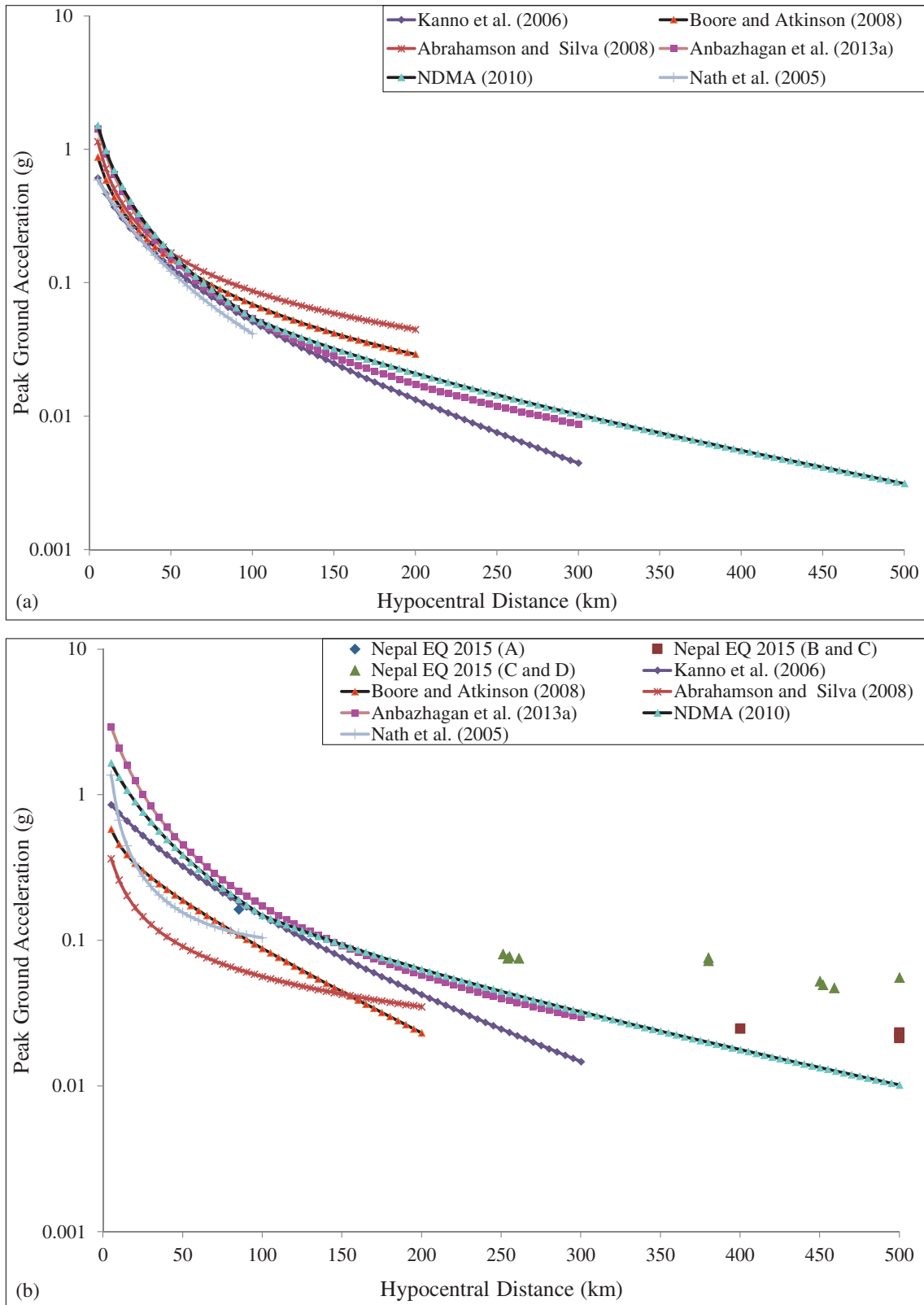


Figure 5. Comparison of ground motion prediction equations used to estimate seismic hazard for earthquake moment magnitude of (a) 6.8 and (b) 7.8 (Nepal 2015 earthquake).

7.1 Deterministic seismic hazard analysis

The worst-case scenario map i.e., deterministic hazard map is required for estimating seismic

vulnerability, seismic losses and for seismic disaster planning and mitigation. Usually, one or more earthquakes are identified by magnitude and location with respect to the site. In this approach,

the earthquake is assumed to occur in the portion of the site or closest to the site. In this study, the worst-case scenario map of the SSA of Kanpur has been prepared considering all the seismic sources lying within the study area and their corresponding maximum magnitudes and the selected GMPEs with different weight factors as explained above. GMPEs were selected and weights were calculated based on regional data as explained earlier (see table 6). A total of 90 seismic sources have experienced an earthquake of moment magnitude 4.0 or above and lies within a 500-km radial distance from Kanpur city center (shown in figure 1). For carrying out the seismic hazard analysis of the Kanpur urban center, the whole city was divided into 635 grids of size $0.02^\circ \times 0.02^\circ$ along the longitude and latitude, respectively. A MATLAB code has been developed for carrying out the DSHA, which has also been verified by manual calculations for Kanpur city center. Using this code, the minimum hypocentral distance has been estimated from the center of each grid to each fault. Thereafter, the PGA from each source at each grid has been estimated considering the maximum magnitude M_{\max} with different weight factors as mentioned above and similarly the selected GMPEs with different weight factors. The maximum PGA from all the seismic sources were assigned as the PGA for that grid. The same procedure was adopted for all the 635 grids and the maximum PGA out of all the grids was taken as the final PGA value for the development of new seismic hazard map of Kanpur city. The Kriging interpolation technique was used for the estimation of the intermediate values of PGA required for the development of the seismic hazard map.

Figure 6(a) shows the worst-case scenario or DSHA map of the Kanpur city center. The PGA variation was found to be 0.04 g in the north-western periphery, whereas it increased to 0.36 g in southern periphery. PGA value in the central part of Kanpur is 2–3 times less as compared to southern part of the city. The high hazard values due to Lucknow–Faridabad fault, which lies near to the city, are a source of devastating earthquakes. In addition to that, spectral acceleration (SA) maps at 0.2 and 1 s were developed and is shown in figure 6(b) and (c). The north-western and north-eastern parts include areas like Araul, Bilhaur, Bithur and surrounding areas, which are less prone to earthquake-induced ground shaking. However, areas that fall in the south and central part of the city such as Bindhu, Ghatampur, Sarli, Narwal and their nearby areas are more susceptible to earthquake shaking. The maximum PGA after carrying out DSHA for the present study has been found to be 0.36 g. Parvez *et al.* (2003) developed a DSHA map for the entire Indian subcontinent and found the range of PGA to be between 0.3 and 0.6 g for the Kanpur city. However, the PGA value found from the present study is higher than that of deterministic seismic hazard macrozonation carried out by Kolathayar *et al.* (2012), which is in the range of 0.15–0.25 g.

7.2 Probabilistic seismic hazard analysis

The probability of exceedance of a given ground motion in a particular time period can be estimated if the probability of its size, locations and level of ground shaking is known cumulatively. The seismic

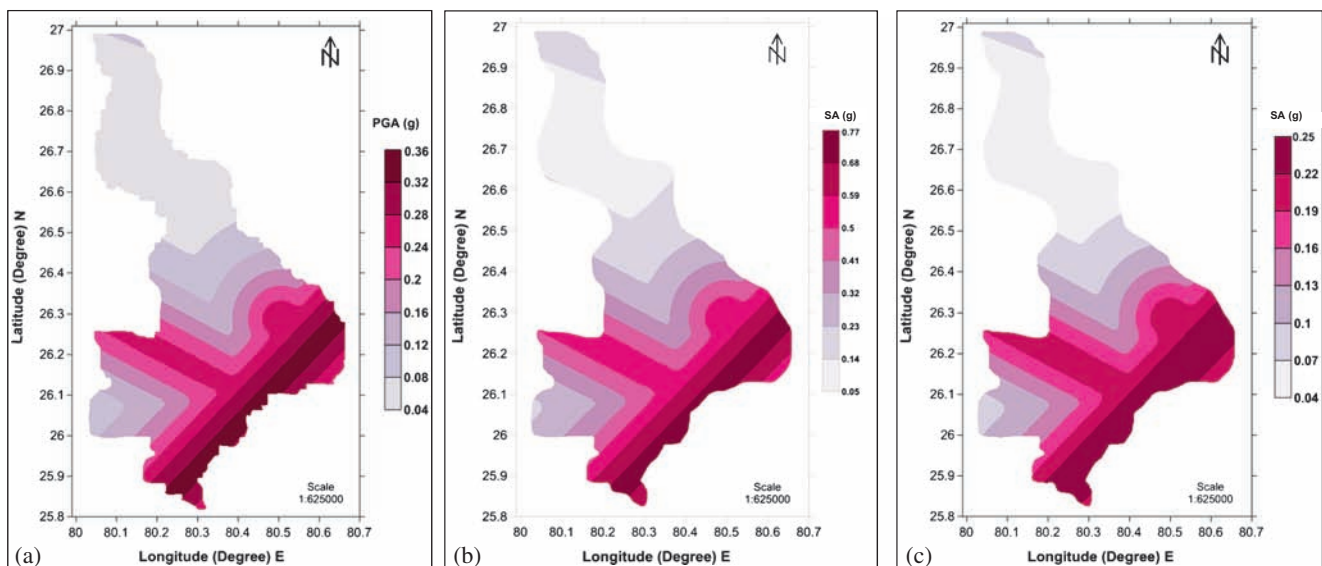


Figure 6. (a) Peak ground acceleration (PGA) map, (b) SA at 0.2 s map of Kanpur urban center, and (c) SA at 1 s of Kanpur urban center.

hazard map for Kanpur city has been generated using PSHA algorithm proposed by Cornell (1968) that was later improved by Algermissen *et al.* (1982). For evaluating the seismic hazard using the classical approach (Cornell 1968), the whole city has been divided into 635 grids of size $0.02^\circ \times 0.02^\circ$ along the longitude and latitude, respectively, similar to DSHA. The uncertainties associated with magnitude, hypocentral distance and the probability of exceedance for GMPEs for 90 seismic sources were computed using a program developed in MATLAB. The program computed the frequency of exceedance of a particular magnitude ' m_i ' occurring at a particular hypocentral distance ' R ' with a known probability of exceedance with respect to ' z ', and the combined frequency of exceedance of a particular ground motion can be estimated by merging all types of uncertainties for each seismic source. The detailed methodology for determining the PGA using probability seismic hazard analysis is explained in Anbazhagan *et al.* (2009).

A hazard curve is defined as the frequency of exceedance of various levels of ground motion. Figure 7 shows the 10 most vulnerable sources at Kanpur city center. It can be seen from figure 7 that F166 is the most vulnerable source located at a hypocentral distance of 10.25 km from city center with a maximum magnitude of 5 (M_w). Other

sources, which were found vulnerable for Kanpur city center, are also shown in figure 7 as F167, F168, F165, F156, F161, F154, F160, F83 and F173. The hazard curve for any SSA can be obtained by the summation of all the hazard curves obtained from all the active sources. Thus, by merging all the hazard curves from the 90 sources at the Kanpur center will give the hazard curve for Kanpur city center. Figure 8 shows the cumulative hazard curve obtained at the Kanpur city center for 0, 0.05, 0.1, 0.2, 0.3, 0.4, 0.6, 0.8, 1.0, 1.6 and 2 s. Hazard curve subsequent to different periods presents the spectral acceleration values for an identified probability of exceedance in a particular time period. In can be observed from figure 8, that the frequency of exceedance for 0.075 g at zero second is 0.0029, which will give a return period of 345 years (return period is the inverse of the frequency of exceedance). This indicates that PGA of 0.075 g has a 13.54% probability of exceedance in 50 years at the Kanpur center. Similarly for 0.5 g, the frequency of exceedance at zero second is $1.12E-05$ which will give a return period of 89.5 thousand years or a probability of exceedance of $5.85 \times 10^{-2}\%$ in 50 years, at Kanpur city center. As the period on interest increases from 0 to 0.8 s, a huge change in return period is observed from figure 8. Initially, the frequency of exceedance decreases from 345

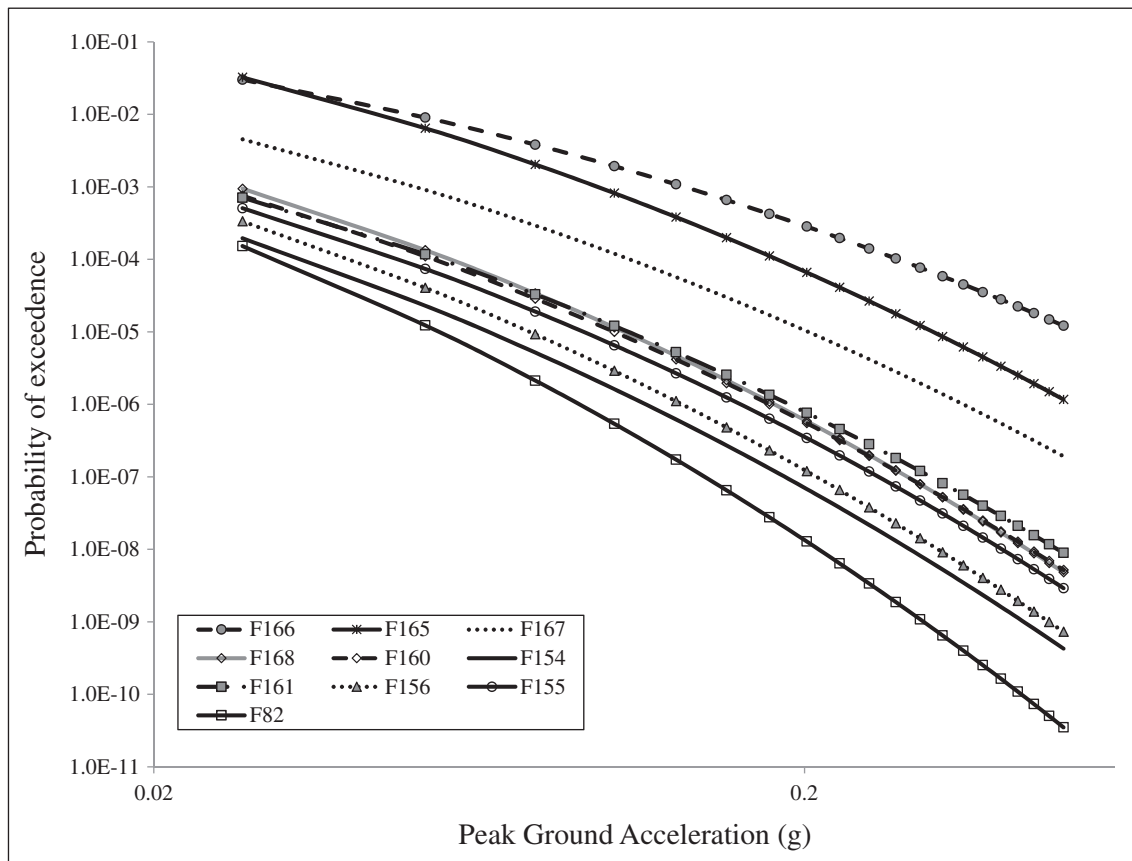


Figure 7. Hazard curve for 10 most contributing seismic sources at Kanpur city center.

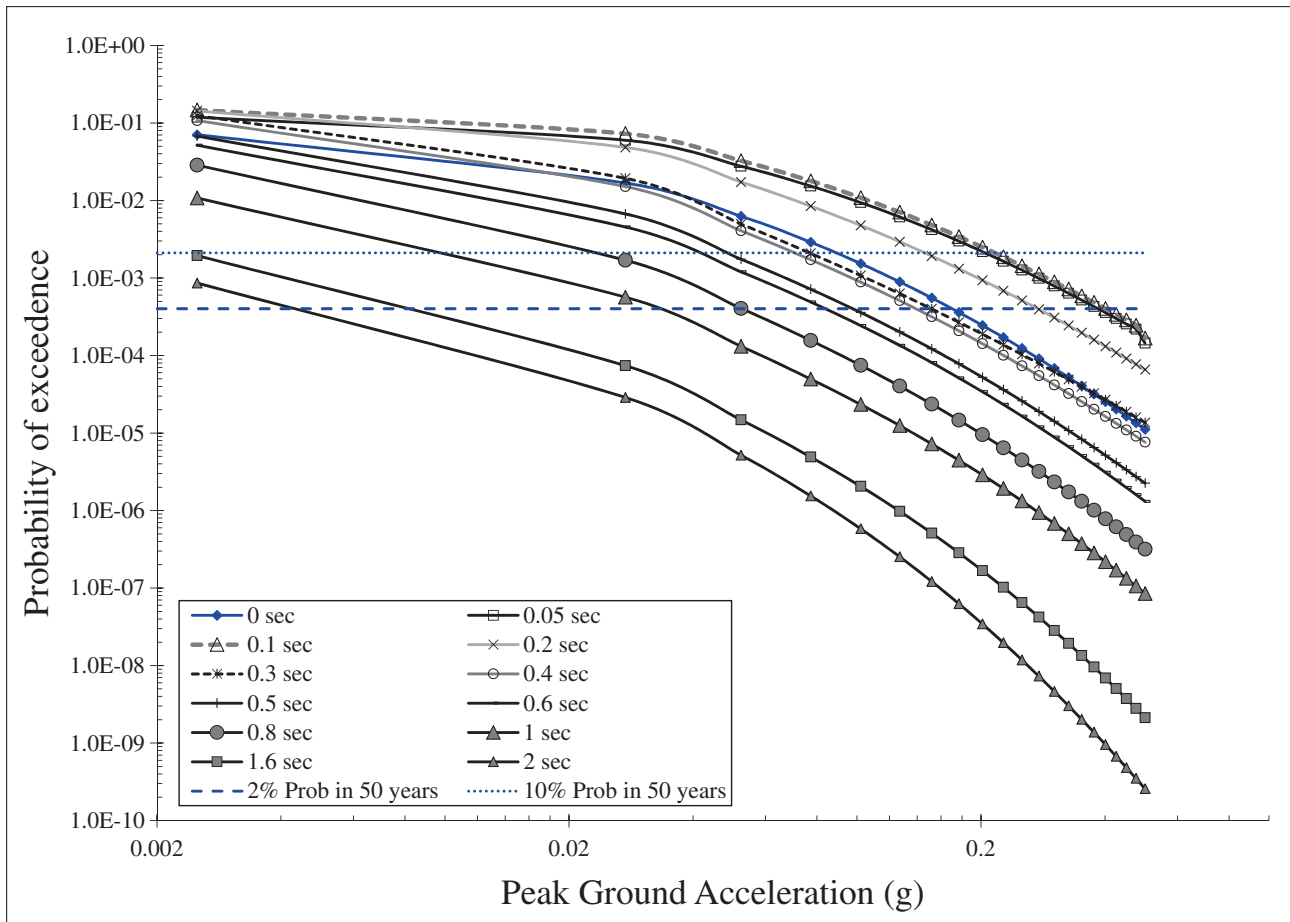


Figure 8. Hazard curve at Kanpur city center for different periods using classical approach.

years at zero periods to 55 years in 0.1 s, which further increases to 118 years in 0.2 s and again till $6.45E+05$ years for 2 s. In order to understand the hazard contribution from various combinations of magnitude and hypocentral distance, degradation plot is generated, which is a function of magnitude and hypocentral distance for all the levels of spectral period associated with the GMPEs. The mean degradation plot for Kanpur SSA for 2% and 10% probability of exceedance at 50 years were made in order to understand the hazard contribution for various magnitudes at a different hypocentral distance and are shown in figure 9(a and b). It has been observed from figure 9 that the motion for $5.5 M_w$ at 20 km hypocentral distance is predominantly for 2% probability of exceedance at 50 years. Similarly, for 10% probability of exceedance at 50 years, the motion for $5.5 M_w$ at 15 km hypocentral distance is predominant. Hazard curve was generated at each grid for Kanpur SSA; the level of ground motion for frequency of exceedance ' $v(z)$ ' can be determined from it. The level of ground motions was estimated from the zero period hazard curves (PGA value) of each grid for 2% and 10% probability of exceedance in 50 years. Figure 10(a) and (b) are the PSHA maps for Kanpur center for

2% and 10% probability of exceedance in 50 years, respectively. It can be observed from figure 10(a) that PGA varies from 0.44 g in the north-western and 0.02 g in the north-western periphery to 0.32 g towards the south-eastern part of the city. PGA value in the south-eastern part of Kanpur is two times as compared to central part of the city. Similarly, for 10% probability of exceedance in 50 years, the PGA value is less at the north-western part of the city and increases about two folds towards the south-eastern part of the city. The north-western and north-eastern parts include areas like Araul, Bilhaur, Bithur and surrounding areas which are less prone to earthquake-induced ground shaking. However, areas that fall in south and central part of the city such as Bindhu, Ghatampur, Sarli, Narwal and their nearby areas are more susceptible to earthquake shaking. Recently, the National Disaster Management Authority (NDMA 2010) and Nath and Thingbaijam (2012) have developed a PSHA map for entire India. Nath and Thingbaijam (2012) predicted the PGA value at Kanpur considering a 10% probability of exceedance in 50 years as 0.12 g, whereas as per NDMA (2010), PGA value at 2% and 10% probability of exceedance for 50 years as 0.08 and 0.04 g, respectively.

As per Khattri *et al.* (1984), the PGA value for Kanpur city center is 0.05 g, as per 10% probability of exceedance in 50 years. Bhatia *et al.*

(1999) presented a PSHA of India under the Global Seismic Hazard Assessment Program (GSHAP) framework. As per Bhatia *et al.* (1999), the PGA

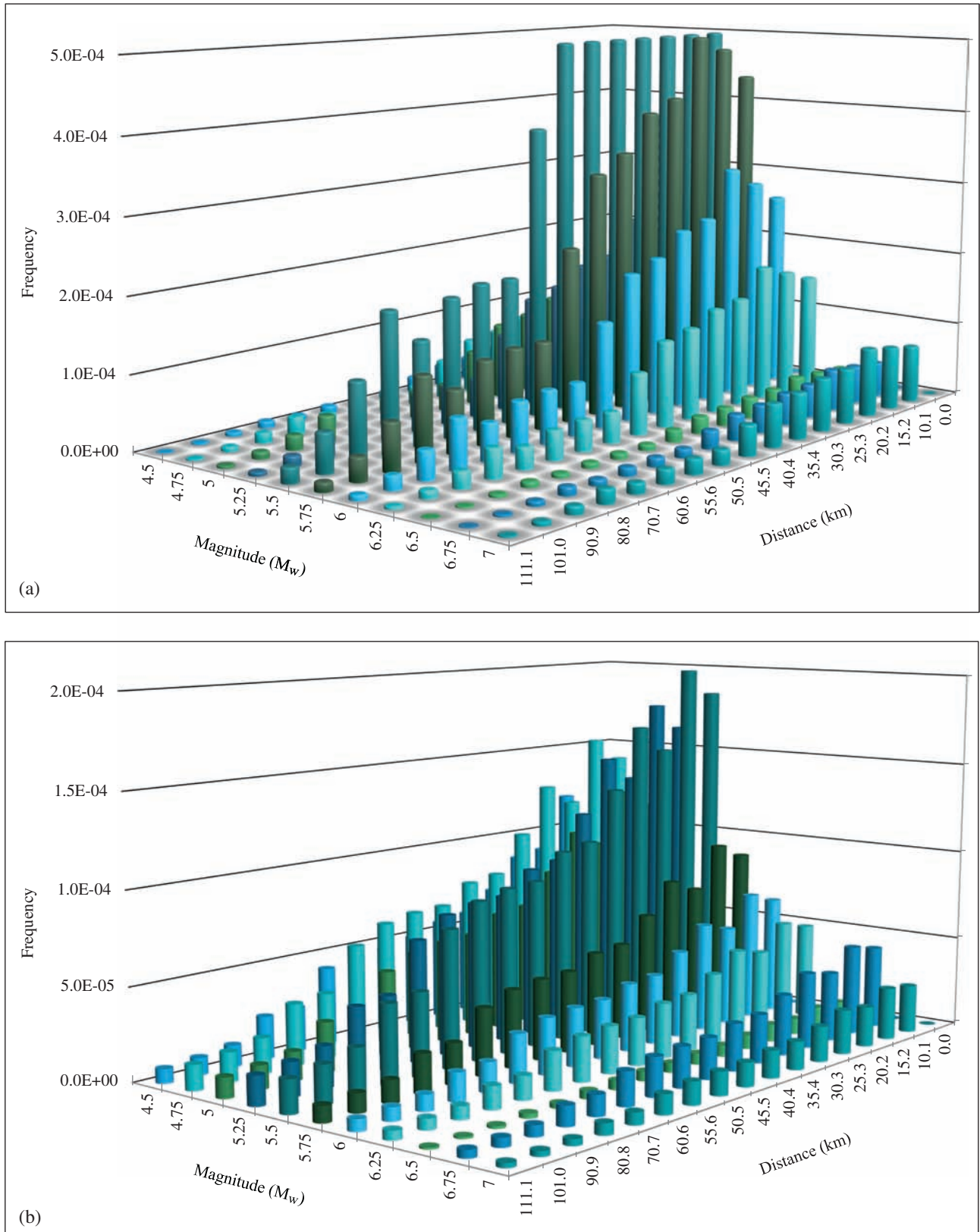


Figure 9. Deaggregation of hazard value at Kanpur city center at bed rock at PGA for (a) 2% and (b) 10% probability of exceedance in 50 years.

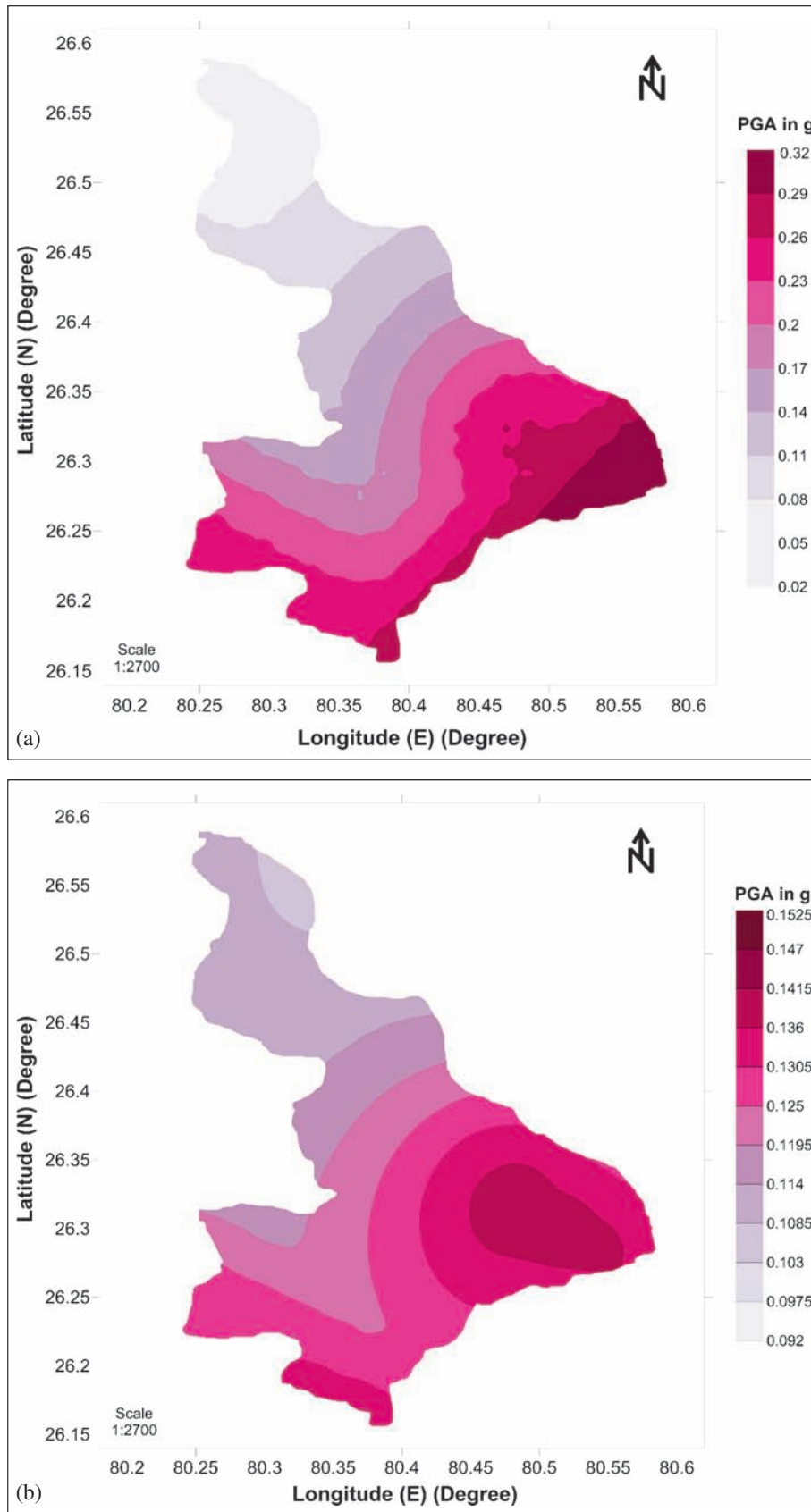


Figure 10. PSHA map for Kanpur city for (a) 2% and (b) 10% probability of exceedance in 50 years.

value is in between 0.05 and 0.1 g of Kanpur city center, considering 10% probability of exceedance in 50 years. As per Yadav *et al.* (2011), the return period of moment magnitude 7 and more is 88.8 years, with a probability of 0.43 and 0.68 in 50 and 100 years, respectively. The predicted PGA value in this study is comparable and slightly higher than the previous studies, it may be due to updated seismicity and considering regional specific maximum magnitude and GMPE.

8. Site-specific spectrum

The site-specific spectrum (SSS) is generally used for the seismic design of structures and to understand the amplification character of the region. In this study, SSS is derived from the above-mentioned GMPE for different segments of the SSA. Three vulnerable seismic sources causing hazard at the central part of Kanpur and spectral acceleration was delineated for deriving the SSS. The seismic

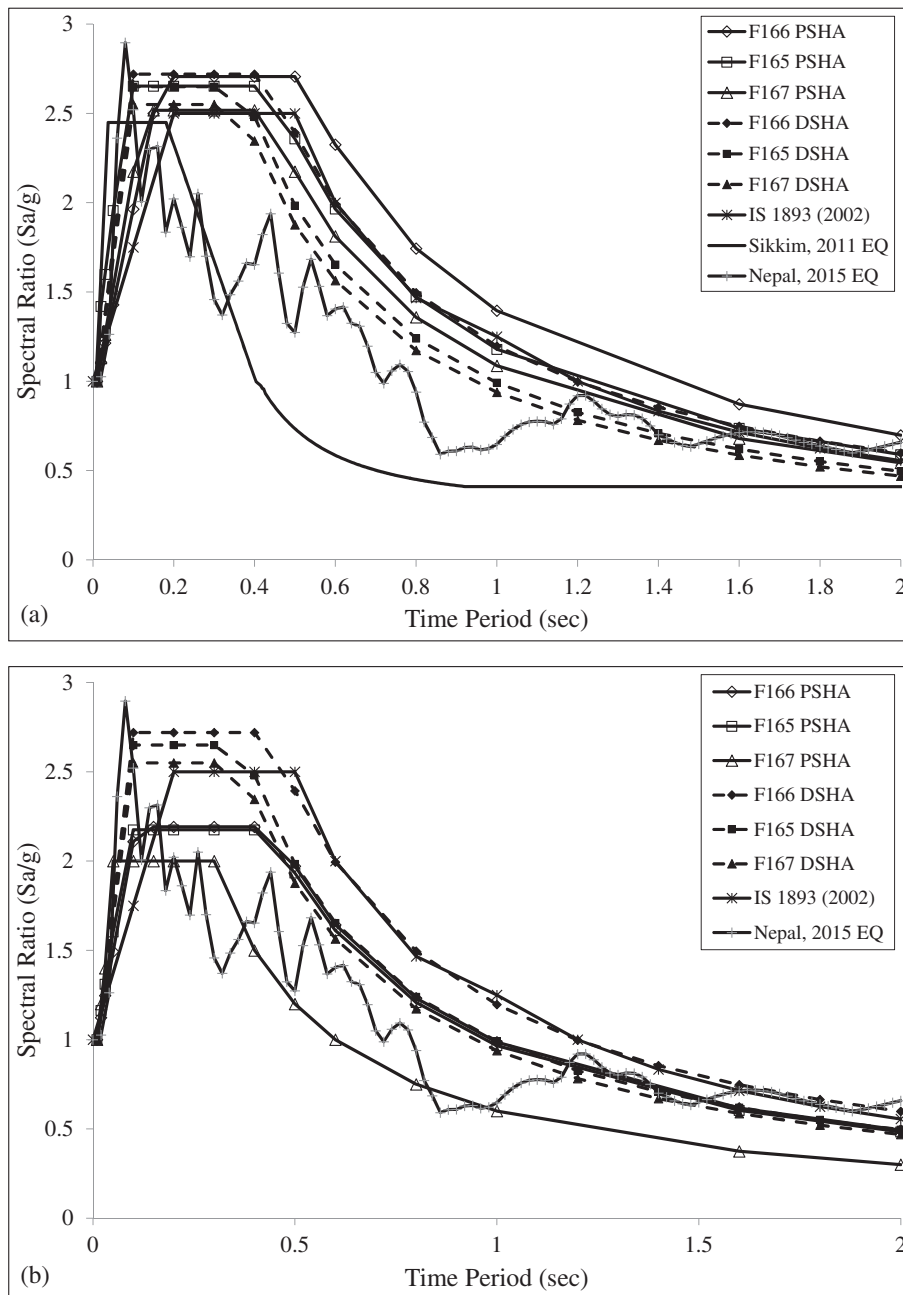


Figure 11. Normalised design spectrum for Kanpur for 5% damping from three vulnerable sources and spectrum from 2011 Sikkim earthquake, 2015 Nepal earthquake and IS 1893 (2002) for (a) 2% and (b) 10% probability of exceedance in 50 years comparing with worst case scenario DSHA result.

sources S166, S165 and S167 are the most vulnerable when compared to other sources. GMPEs ABSI-08, ANBU-13, NDMA-10, KANO-06, NATH-05 and BOAT-08 are used up to a hypocentral distance of 100 km. For 100–300 km distance, KANO-06, ANBU-13, NDMA-10 and BOAT-10 and for a hypocentral distance greater than 300 km, NDMA-10 are used for deriving SSS (see table 6). Spectral coefficients are the function of period for respective GMPEs at 5% damping and were taken from respective published research papers. The NATH-05 GMPE was not used in deriving SSS in this study, as it does not have spectral coefficients for different periods. Maximum and minimum smoothed spectrums from each GMPE have been evaluated considering these three vulnerable sources. Averaged smoothed spectrum from maximum and minimum smoothed spectra has been developed as per Malhotra (2006). The smoothed spectrum comprises a peak, valley and shape variation in response to spectrum from each GMPE. The smooth spectra was developed by normalising the SA value at a different period with respect to SA at zero periods (PGA) and given as spectral ratio *vs.* period.

Figure 11(a) and (b) also show the normalised uniform hazard spectrum for 5% damping considering DSHA values and PSHA with IS code and Sikkim and Nepal earthquake spectrum comparison. This can be considered as the site-specific normalised design spectrum curve for 5% damping at the rock level for considering three venerable sources at the center of Kanpur city. These rock level normalised design spectrums were compared with the Sikkim earthquake 2011 recorded at Gangtok seismic station, located at rock site and with Nepal 2015 with a station located at soil site. It can be observed from figure 11(b) that up to 0.2 s, the spectral values are more than the IS code, from 0.2 to 1.2 less than the IS code, and after 1.2 s, matching with the IS code. It has been seen that the present DSHA design spectrum is predicting slightly higher value than recorded values and 2% probability of exceedance in 50 years (see figure 11). Site-specific spectrum developed for Kanpur city is also compared with the design spectrum of IS-1893 (2002) of soil category of type I (rock or hard soil). The value of spectral acceleration developed for 2% probability of exceedance in 50 years from the present study is equal for F167 and higher for F166 and F165, when compared with IS-1893 (2002). Moreover, it is also higher in the case of DSHA and lower, while considering PSHA with 10% probability of exceedance in 50 years, when considering these three vulnerable sources. This may be because IS-1893 (2002) deals on a macro level (see figure 11a) and the present study is in micro level and region specific. It has been observed that the normalised design spectra developed in

this study, both deterministically and probabilistically, is either higher or lower as compared to IS-code. This might be due to the incorporation of regional specific parameters and using site-specific GMPE and maximum magnitude.

9. Conclusion

This paper presents the seismic hazard map and site-specific design spectrum for Kanpur city, considering both deterministic and probabilistic approaches along with region-specific data. A seismic study area of 500 km was considered based on past earthquake damage distribution and a seismotectonic map was generated. The seismotectonic map consists of declustered and homogenised past earthquake data and all the linear sources. The maximum magnitude was estimated by considering four methods, i.e., the maximum observed magnitude, incremental method, Kijko method and regional rupture-based characteristic method. The maximum magnitude at each source was selected by analysing the error and uncertainty in all the methods, hence, different weight factors were assigned to these values calculated using these methods. About 27 GMPEs are applicable to the study region and suitable GMPEs are identified by performing the efficacy test. The segment-based efficacy test was carried out and GMPEs were selected based on the same. Six GMPEs such as ABSI-08, ANBU-13, NDMA-10, KANO-06, NATH-05 and BOAT-08 were used up to a hypocentral distance of 100 km. For 100–300 km distance, KANO-06, ANBU-13, NDMA-10 and BOAT-10 were used and for a hypocentral distance >300 km, NDMA-10 was used for hazard analysis. Hazard curve for 0, 0.05, 0.1, 0.2, 0.3, 0.4, 0.6, 0.8, 1.0, 1.6 and 2 s were also generated. The hazard maps for both 2% and 10% probability of exceedance in 50 years were developed. PGA varied from 0.04 to 0.36 g for DSHA, from 0.02 to 0.32 g in case for 2% probability and from 0.092 to 0.153 g for 10% probability in 50 years. Furthermore, site-specific design spectrum developed using DSHA is comparable with 2% probability of exceedance in 50 years; however, it is either low or high when compared to IS-code for DSHA, as well as PSHA. The present result is more region specific and advanced than previous studies and can be further used for estimating microzonation parameter of Kanpur district. Seismic hazard values given in this paper are at rock condition with $V_s^{30} > 1500$ m/s. These values may alter when site effects based on site-specific soil properties are considered.

Acknowledgements

The authors would like to thank the editor and the anonymous reviewers for their comments to

improve the manuscript. The authors extend their sincere appreciations to the Deanship of Scientific Research at King Saud University for its funding this Prolific Research Group (PRG-1436-06).

References

- Abrahamson N A and Litehiser J J 1989 Attenuation of vertical peak accelerations; *Bull. Seismol. Soc. Am.* **79** 549–580.
- Abrahamson N A and Silva W J 2007 Abrahamson & Silva NGA ground motion relation for the geometric mean horizontal component of peak and spectral ground motion parameters; Pacific Earthquake Engineering Research Center Report, College of Engineering, University of California, Berkeley.
- Abrahamson N A and Silva W J 2008 Summary of the Abrahamson & Silva NGA ground motion relations; *Earthq. Spectra* **24** 67–97.
- Aghabarati H and Tehranizadeh 2009 Near-source ground motion attenuation relationship for PGA and PSA of vertical and horizontal components; *Bull. Earthq. Eng.* **7** 609–635, doi: 10.1007/s10518-009-9114-9.
- Akkar S and Bommer J J 2010 Empirical equations for the prediction of PGA, PGV and spectral acceleration in Europe, the Mediterranean region and the Middle East; *Seismol. Res. Lett.* **81** 195–206.
- Algermissen S T, Perkins D M, Thenhaus P C, Hanson S L and Bender B L 1982 Probabilistic estimates of maximum acceleration and velocity in rock in the contiguous United States; Open File Report 82–1033 USGS, Washington DC 99.
- Ambraseys N and Douglas J S 2004 Magnitude calibration of north Indian earthquakes; *Geophys. J. Int.* **159** 165–206.
- Ambraseys N, Douglas J S, Sarma K and Smit P M 2005 Equation for the estimation of strong ground motions from shallow crustal earthquakes using data from Europe and the Middle East: Horizontal peak ground acceleration and the spectral acceleration; *Bull. Earthq. Eng.* **3** 1–53.
- Anbazhagan P, Vinod J S and Sitharam T G 2009 Probabilistic seismic hazard analysis for Bangalore; *Nat. Hazards* **481** 45–166.
- Anbazhagan P, Kumar A and Sitharam T G 2013a Ground motion prediction equation considering combined data set of recorded and simulated ground motions; *Soil Dyn. Earthq. Eng.* **53** 92–108.
- Anbazhagan P, Smitha C V, Kumar A and Chandran D 2013b Seismic hazard assessment of NPP site at Kalpakkam, Tamil Nadu, India; *Nucl. Eng. Des.* **259** 41–64.
- Anbazhagan P, Bajaj K, Moustafa S S R and Al-Arifi N S 2015a Maximum magnitude estimation considering the regional rupture characteristics; *J. Seismol.* **19**(3) 695–719.
- Anbazhagan P, Bajaj K and Patel S 2015b Seismic hazard mapping and spectrum for Patna considering region specific seismotectonic parameters; *J. Nat. Hazards*, doi: 10.1007/s11069-015-1764-0.
- Anbazhagan P, Sreenivas M, Bajaj K, Moustafa S S R and Al-Arifi N S 2016 Selection of ground motion prediction equation for seismic hazard analysis of peninsular India; *J. Earthq. Eng.*, doi: 10.1080/13632469.2015.1104747.
- ASC (Amateur Seismic Centre) 2010 Seismicity of Uttar Pradesh; <http://asc-india.org/seismi/seis-uttar-pradesh.htm>.
- Atkinson G and Boore D M 2003 Empirical ground-motion relations for subduction-zone earthquakes and their application to Cascadia and other regions; *Bull. Seismol. Soc. Am.* **93** 1703–1729.
- Atkinson G M and Boore D M 2006 Earthquake ground-motion prediction equations for eastern North America; *Bull. Seismol. Soc. Am.* **96** 2181–2205.
- Baruah S, Gogoi N K, Erteleva Q, Aptikaev F and Kayal J R 2009 Ground motion parameters of Shillong plateau: One of the most seismically active zones of northeastern India; *Earthq. Sci.* **22** 283–291.
- Bhatia S C, Ravi M K and Gupta H K 1999 A probabilistic seismic hazard map of India and adjoining regions; *Ann. Geofis.* **42** 1153–1164.
- Bilham R 2015 Rising Kathmandu; *Natural Geosci.* **8**(8) 582–584.
- Bommer J J, Douglas J, Scherbaum F, Cotton F, Bungum H and Fäh D 2010 On the selection of ground-motion prediction equations for seismic hazard analysis; *Seismol. Res. Lett.* **81**(5) 783–793.
- Boore D M and Atkinson G M 2008 Ground-motion prediction equations for the average horizontal component of PGA, PGV and 5% damped PSA at spectral periods between 0.01 and 10.0 s; *Earthq. Spectra* **24**(1) 99–138.
- Campbell K W 1997 Empirical near-source attenuation relationships for horizontal and vertical components of peak ground acceleration, peak ground velocity and pseudo-absolute acceleration response spectra; *Seismol. Res. Lett.* **68**(1) 154–179.
- Campbell K W and Bozorgnia Y 2006 Next generation attenuation relation (NGA) empirical ground motion models: Can they be used for Europe; In: *Proceedings of first European conference on earthquake engineering and seismology*, Geneva, Switzerland, 458p.
- Campbell K W and Bozorgnia Y 2008 NGA ground motion model for the geometric mean horizontal component of PGA, PGV, PGD and 5% damped linear elastic response spectra for period ranging from 0.01 to 10 s; *Earthq. Spectra* **24** 139–171.
- Chadha R K, Srinagesh D, Srinivas D, Suresh G, Sateesh A, Singh S K, Pérez-Campos X, Suresh G, Koketsu K, Masuda T, Domen K and Ito T 2016 CIGN, A strong-motion seismic network in Central Indo-Gangetic Plains, foothills of Himalayas: First results; *Seismol. Res. Lett.* **87**(1) 37–46.
- Cornell C A 1968 Engineering seismic risk analysis; *Bull. Seismol. Soc. Am.* **58** 1583–1606.
- Das S, Gupta I D and Gupta V K 2006 A probabilistic seismic hazard analysis of northeast India; *Earthq. Spectra* **22** 1–27.
- Delevald E, Scherbaum F, Kuehn N and Riggelsen C 2009 Information-theoretic selection of ground motion prediction equations for seismic hazard analysis: An applicability study using Californian data; *Bull. Seismol. Soc. Am.* **99** 3248–3263.
- Delevald E, Scherbaum F, Kuehn N and Allen T 2012 Testing the global applicability of ground-motion prediction equations for active shallow crustal regions; *Bull. Seismol. Soc. Am.* **102**(2) 702–721.
- EERI Committee on Seismic Risk 1984 Glossary of terms for probabilistic seismic-risk and hazard analysis; *Earthq. Spectra* **1** 33–36.
- EM-1110 1999 Engineer manual 1110–2-6050 Department of Army, U.S. Army Corps of Engineers, Washington DC-20314–1000.
- Frankel A 1995 Mapping seismic hazard in the central eastern United States; *Seismol. Res. Lett.* **66**(4) 8–21.
- Gardner J K and Knopoff L 1974 Is the sequence of earthquakes in southern California, with aftershocks removed, Poissonian; *Bull. Seismol. Soc. Am.* **64**(5) 1363–1367.
- Grünthal G 1998 European macroseismic scale; *Cahiers du Centre Européende Géodynamiqueet de Séismologie*, vol. **15**.

- GSI 2000 Eastern Nepal–Himalaya and Indo-Gangetic plains of Bihar; In: Seismotectonics atlas of India and its environs (eds) Narula P L, Acharyya S K and Banerjee J, *Geol. Surv. India*, pp. 26–27.
- Gutenberg B and Richter C F 1956 Earthquake magnitude, intensity, energy and acceleration; *Bull. Seismol. Soc. Am.* **46** 105–145.
- Gupta I D 2010 Response spectral attenuation relations for inslab earthquakes in Indo-Burmese subduction zone; *Soil Dyn. Earthq. Eng.* **30** 368–377.
- IAEA SGS-9 2010 Seismic hazards in site evaluation for nuclear installations; http://www-pub.iaea.org/MTCD/publications/PDF/Pub1448_sweb.pdf.
- Idriss I M 2008 An NGA empirical model for estimating the horizontal spectral values generated by shallow crustal earthquakes; *Earthq. Spectra* **16** 363–372.
- IS 1893 2002 Indian standard criteria for earthquake resistant design of structures. Part 1: General provisions and buildings: Bureau of Indian Standards, New Delhi.
- Joshi G C and Sharma M L 2008 Uncertainties in the estimation of M_{\max} ; *J. Earth Syst. Sci.* **117(S2)** 671–682.
- Kayal J R 2008 *Microearthquake seismology and seismotectonics of South Asia*; Springer, N Y co-published with Capital Publishing Company, India.
- Kaklamanos J and Baise L G 2011 Model validations and comparisons of the next generation attenuation of ground motions (NGA–West) project; *Bull. Seismol. Soc. Am.* **101(1)** 160–175.
- Kanno T, Narita A, Morikawa N, Fujiwara H and Fukushima Y 2006 A new attenuation relation for strong ground motion in Japan based on recorded data; *Bull. Seismol. Soc. Am.* **96** 879–897.
- Khattari K N, Rogers A M, Perkins D M and Algermissen S T 1984 A seismic hazard map of India and adjacent areas; *Tectonophysics*. **108** 93–134.
- Kijko A and Sellevoll M A 1989 Estimation of earthquake hazard parameters from incomplete data files: Part I. Utilization of extreme and complete catalogues with different threshold magnitudes; *Bull. Seismol. Soc. Am.* **79** 645–654.
- Kolathayar S, Sitharam T G and Vipin K S 2012 Deterministic seismic hazard microzonation of India; *J. Earth Syst. Sci.* **121** 1351–1364.
- Kumar S 2012 Seismicity in the NW Himalaya India: Fractal dimension, b-value mapping and temporal variation for hazard evaluation; *Geosci. Res.* **3(1)** 83–87.
- Kumar A, Anbazhagan P and Sitharam T G 2013 Seismic hazard analysis of Lucknow considering local and active seismic gaps; *Nat. Hazards* **69** 327–350.
- Lin P S and Lee C H 2008 Ground-motion attenuation relationship for subduction-zone earthquakes in northeastern Taiwan; *Bull. Seismol. Soc. Am.* **98(1)** 220–240.
- Mahajan A K, Thakur V C, Sharma M L and Chauhan M 2010 Probabilistic seismic hazard map of NW Himalaya and its adjoining area, India; *Nat. Hazards* **53** 443–457.
- Malhotra P K 2006 Smooth spectra of horizontal and vertical ground motions; *Bull. Seismol. Soc. Am.* **96(2)** 506–518.
- Nadesha 2004 Lucknow is on earthquake list; <http://timesofindia.indiatimes.com/city/lucknow/Lucknow-is-onearthquakelist/articleshow/679471.cms>.
- Nath S K and Thingbaijam K K S 2011 Peak ground motion predictions in India: An appraisal for rock sites; *J. Seismol.* **15** 295–315.
- Nath S K and Thingbaijam K K S 2012 Probabilistic seismic hazard assessment of India; *Seismol. Res. Lett.* **83** 135–149.
- Nath S K, Vyas M, Pal I and Sengupta P 2005 A hazard scenario in the Sikkim Himalaya from seismotectonics spectral amplification source parameterization and spectral attenuation laws using strong motion seismometry; *J. Geophys. Res.* **110** 1–24.
- Nath S K, Raj A, Thingbaijam K K S and Kumar A 2009 Ground motion synthesis and seismic scenario in Guwahati city: A stochastic approach; *Seismol. Res. Lett.* **80(2)** 233–242.
- NDMA 2010 Development of probabilistic seismic hazard map of India; Technical Report by National Disaster Management Authority, Government of India.
- Parvez I A, Vaccari F and Panza G F 2003 A deterministic seismic hazard map of India and adjacent areas; *Geophys. J. Int.* **155** 489–508.
- Reasenber P 1985 Second-order moment of central California seismicity 1969–1982; *J. Geophys. Res.* **90** 5479–5495.
- Scherbaum F, Delavaud E and Riggelsen C 2009 Model selection in seismic hazard analysis: An information theoretic perspective; *Bull. Seismol. Soc. Am.* **99** 3234–3247.
- Scordilis E M 2006 Empirical global relations converting MS and mb to moment magnitude; *J. Seismol.* **10** 225–236.
- Shanker D and Sharma M L 1998 Estimation of seismic hazard parameters for the Himalayas and its vicinity from complete data files; *Pure Appl. Geophys.* **152** 267–279.
- Sharma M L 1998 Attenuation relationship for estimation of peak ground horizontal acceleration using data from strong motions arrays in India; *Bull. Seismol. Soc. Am.* **88** 1063–1069.
- Sharma M L and Bungum H 2006 New strong ground motion spectral acceleration relation for the Himalayan region; In: *First European Conference on Earthquake Engineering and Seismology*, p. 1459.
- Sharma M L, Douglas J, Bungum H and Kotadia J 2009 Ground-motion prediction equations based on data from Himalayan and Zagros regions; *J. Earthq. Eng.* **13** 1191–1210.
- Singh R P, Aman A and Prasad Y J J 1996 Attenuation relations for strong ground motion in the Himalayan region; *Pure Appl. Geophys.* **147** 161–180.
- Spudich P, Joyner W B, Lindh A G, Boore D M, Margaritis B M and Fletcher J B 1999 SEA99: A revised ground motion prediction relation for use in extensional tectonic regions; *Bull. Seismol. Soc. Am.* **89(5)** 1156–1170.
- Sreevalsa K, Sitharam T G and Vipin K S 2011 Spatial variation of seismicity parameters across India and adjoining area; *Nat. Hazards*, doi: 10.1007/s11069-011-9898-1.
- Stapp J C 1972 Analysis of completeness of the earthquake sample in the Puget sound area and its effect on statistical estimates of earthquake hazard; In: *Proc. Int. Conf. Microzonation, Seattle, October 30–November 3, 1972* **2** 897–910.
- Stiphout V T, Zhuang J and Marsan D 2010 Seismicity declustering; *Community Online Resource for Statistical Seismicity Analysis*; <http://www.corssa.org>.
- Takahashi T, Saiki T, Okada H, Irikura K, Zhao J X, Zhang J, Thoi H K, Somerville P G, Fukushima Y and Fukushima Y 2004 Attenuation models for response spectra derived from Japanese strong-motion records accounting for tectonic source types; In: *13th World Conference of Earthquake Engineering*, Vancouver, B.C., Canada, paper 1271.
- Uhrhammer R A 1986 Characteristics of northern and central California seismicity; *Earthquake Notes* **1** 21.
- Wells D L and Coppersmith K J 1994 New empirical relationships among magnitude, rupture length,

- rupture width, rupture area and surface displacement; *Bull. Seismol. Soc. Am.* **4(84)** 975–1002.
- Wiemer S and Wyss M 1994 Seismic quiescence before the Landers ($M = 7.5$) and Big Bear ($M = 6.5$) 1992 earthquakes; *Bull. Seismol. Soc. Am.* **84** 900–916.
- Wiemer S and Wyss M 1997 Mapping the frequency-magnitude distribution in asperities: An improved technique to calculate recurrence times; *J. Geophys. Res.* **102** 15,115–15,128.
- WGCEP (Working Group on Central California Earthquake Probabilities) 1995 Seismic hazard in Southern California: Probable earthquakes 1994 to 2024; *Bull. Seismol. Soc. Am.* **85** 379–439.
- Yadav R B S, Bayrak Y, Tripathi J N, Chopra S, Singh A P and Bayrak E 2011 A probabilistic assessment of earthquake hazard parameters in NW Himalayan and adjoining regions; *Pure Appl. Geophys.* **169** 1619–1639.
- Youngs R R, Chiou S J, Silva W J and Humphrey J R 1997 Strong ground motion relationship for subduction earthquakes; *Seismol. Res. Lett.* **68** 58–73.
- Zhao J X, Zhang J, Asano A, Ohno Y, Oouchi T, Takahashi T, Ogawa H, Irikura K, Thio H K, Somerville P G, Fukushima Y and Fukushima Y 2006 Attenuation relations of strong ground motion in Japan using site classification based on predominant period; *Bull. Seismol. Soc. Am.* **96** 898–913.

MS received 28 October 2015; revised 24 June 2016; accepted 7 October 2016

Corresponding editor: N PURNACHANDRA RAO